Capillary electrophoretic apparatus for the endpoint detection in microtitration methods

Farid Oukacine, Luc Choisnard, Annabelle Gèze, Eric Peyrin

Capillary electrophoretic apparatus for the endpoint detection in microtitration methods.

Farid Oukacine*, Luc Choisnard, Annabelle Gèze, and Eric Peyrin
Univ. Grenoble-Alpes, DPM, CNRS UMR 5063, F-38041 Grenoble, France

E-mail: farid.oukacine@univ-grenoble-alpes.fr

ABSTRACT

Titration methods are routinely used in the laboratories for the quantification of acids and bases, for the complexometric determination of metal ions and for the ion-pair titrations of drugs in pharmaceutical control. They also find application in a wide variety of chemical and biochemical studies. However, conventional titration methods (CTM) requires large amounts of samples that are not always available. In absence of micro-titrator devices, the application of these methods for expensive samples and for small batch sizes is not possible. In this work, it was demonstrated that the commercial capillary electrophoretic apparatus (CEa) can be used, in a quick and easy way, for the end-point detection in a microtitration process. The proposed methodology exploits the change of the solutions conductivity during the titrations. The equivalent points can be easily located by plotting the change in electrical current as a function of the titrant volume added. More interestingly, only 1.1−1.5 mL of analyte solutions are required to establish the titration curves. The advantages and the limitations of the procedure are discussed in detail.

Keywords

Capillary electrophoretic apparatus, Ohm's law, microtitration, quantification.

1. Introduction

Capillary electrophoresis (CE) is a separating technique that plays an important role in contemporary analytics. This analytical method is routinely used for the separation of small inorganic ions [1], biomolecules [2], polymers [3], nanoparticles [4], and even bacteria [5] and viruses [6]. CE provides several advantages including very high separation efficiencies, short analysis times and low sample consumption. CE has shown particularly useful for the

study of (bio)molecular interactions [7], analysis of protein-based pharmaceutical and quality controls [2] and in the chiral separation field [8]. Moreover, CEa can be used for a wide range of other applications. For example, it is suitable for the nanoparticle size measurements [9], for the determination of the critical micelle concentration (CMC) of surfactants [10], for the measurement of the viscosities and conductivities of ionic liquids [11]. An ability to perform on-line micro-reactions is a further advantage afforded by CEa [12]. These examples are not exhaustive and a large number of other ones are available in the literature.

In this report, it is demonstrated that the CEa can also be used, with high confidence, for the end-point detection in microtitration methods. Conventional titration methods (CTM) are frequently used in the laboratories for the quantification of acids and bases, for the complexometric determination of metal ions and for the ion-pair titrations of drugs in pharmaceutical control. They also have applications in a wide variety of chemical and biochemical studies [13]. For example, titration methods are frequently applied/implemented on modified celluloses for determining the degree of substitution of the carboxylate groups [14], for the charge density quantification of polyelectrolytes [15], for determining the concentration of amino, carboxyl or hydroxyl groups at the surface of nanomaterials [16]. Unfortunately, CTM require large amounts of samples that are not always available [17]. Then, in the absence of micro-titrator devices, the application of the CTM for expensive samples and for small batch sizes is not possible.

The microtitration method developed in this work, exploits the change of the solutions conductivity (κ) during the titration process. Assuming that the Faradaic current is negligible and the temperature of the electrolyte is perfectly controlled, the measured current intensity (I) in CE is a function of κ according to the following equation [10,11]:

$$I = \kappa\left(\frac{\pi R_C^2 V}{L}\right) \quad (1)$$

were R_c is the capillary radius, L is the capillary length and V is the applied voltage. Based on the fact that I is a function of κ; the electrical current variation during the course of titration can provide interesting informations about the location of the equivalence points (EPs). For the proof of concept, we mainly focus on the acid-base systems commonly encountered in the laboratories. Indeed, due to their low cost, it is easily possible to use large sample volumes to compare the titration curves obtained by CTM (using 100 mL sample volume) with those derived from CEa (using ~1 mL sample volume). This helps to identify the advantages, the drawbacks and the limitations of the method. Moreover, various shapes of titration curves can

be obtained with these models. Once validated, this methodology can potentially be transposed to any other compounds (e. g. nanoparticles, macromolecules…). In this work, 17 acid-base systems characterized either by one or two titratable groups were studied. Important recommendations for the reliability of the results are provided. The advantages and the drawbacks of the procedure are discussed in detail.

2. Experimental

2.1 Chemicals and materials

Tris ($NH_2C(CH_2OH)_3$) and potassium bromide (KBr) were purchased from Sigma-Aldrich (Saint-Quentin, France). Sodium hydroxide (NaOH), hydrochloric acid (HCl), acetic acid (CH_3COOH), ethanol (EtOH) and ammonium hydroxide (containing 28% of NH_3) were provided by Carlo Erba (Val de Reuil, France). Piperidine ($C_5H_{11}N$), oxalic acid (HO_2CCO_2H) and potassium chloride (KCl) were from VWR (Fontenay-sous-Bois, France). Nicotinic acid ($C_6H_5NO_2$) and diethanolamine ($HN(CH_2CH_2OH)_2$) were purchased from Fisher Scientific SAS (Illkirch, France). Purification of water (18.2 MΩ cm) was performed with a Millipore Direct-Q® 3 UV system (Merck Millipore, Guyancourt, France). The 0.2 mL PCR tubes were from VWR (Leuven, Belgium). The injection vials with 0.25 mL capacity were from Agilent Technologies (Ref. 9301-097, Les Ulis, France). All measurements of weight were carried out using Sartorius MSA6.6S-000-DM microbalance (Sartorius AG, Goettingen, Germany).

2.2 Measurement of the current intensities using CEa

The analysis were carried out with an Agilent G1600 3D-CE instrument (Agilent Technologies, Waldbronn, Germany) equipped with a diode array detector. Bare-fused silica capillaries were purchased from Photon Lines (Saint-Germain-en-Laye, France). New fused silica capillary (33 cm of totally length (24.5 cm to the detector) and 50 µm i.d.) was flushed by H_2O during 20 min (at 1 bar). During this step, two vials containing 0.65 and 0.50 µL of water were positionned at the inlet and at the outlet side of the capillary to ensure the cleaning of the electrodes. After that, the capillary was dried with air (10 min at 1 bar) by positionning empty vials at both sides of the capillary. The same washing process was performed between

each sequence and at the end of each day. The detailed acid-base microtitration procedure is depicted in Fig. 1. Briefly, 100 ± 1 µL aliquots of sample were transferred into 0.2 mL PCR tubes. Then, different volumes of titrant were added in each tube using a monochannel pipettes (P2.5 or P10, Gilson, France).

The PCR tubes were stirred vigorously to ensure efficient mixing of the solutions. Test tubes were weighed between each step to determine the precise volumes of sample and titrant loaded. In all cases, the density of solutions were assumed the same as water. Finally, the content of each PCR tube was transferred into two injection vials (50 µL in each vial). The analysis were performed under constant voltage (- 2 kV during 1 min) with both vials at the inlet and at the outlet side of the capillary. Samples were analyzed in sequence mode. The samples were analyzed one after the other in increasing order of titrant volumes. The washing process between runs was performed at 1 bar, during 0.5 min, by positioning injection and empty vials at the inlet and at the outlet side of the capillary, respectively. All the analysis were performed under constant voltage (- 2 kV during 1 min) with two injection vials at both end of the capillary. The temperature of the capillary cartridge was set at 25°C and the electrode offset was maintained at 3 mm.

The treatment of the capillary with NaOH, commonly used in capillary electrophoresis [18], is forbidden in this method. Indeed, if residual NaOH is present in the space between capillary and electrode, it can contaminate samples. The recorded electric current will be not exploitable. For the same purpose, it is also recommended to dry the capillary with air (10 min at 1 bar) before each sequence to prevent the contamination of the samples by the residual water present at the inlet end of the capillary.

2.4 Conventionnal conductometric titrations

Conventionnal conductometric titrations (CCT) were performed using compact precision handheld meter Cond 330i (WTW, Weilheim, Germany) equipped with tetraCon® 325/S conductivity cell (K_{cell} 0.491 cm^{-1}). Briefly, 100 mL of sample solution was transferred to a beaker and the conductivity cell was immersed. Titrant was added from a graduated burette and the conductivity was measured after each addition of titrant solution. Titrations were performed at room temperature and under constant stirring. The conductivities reading were corrected for dilution by using Eq. (2) [19]:

$$\kappa_{corr.} = \kappa\left(\frac{V_0 + V_a}{V_0}\right) \quad (2)$$

were $\kappa_{corr.}$ is the corrected conductivity, κ is the observed conductivity, V_0 is the initial volume of the titrated solution and V_a the titrant added volume.

3. Results and discussion

As discussed in the first section, the aim of this work was to investigate the use of the CEa for the endpoint detection in microtitration methods. Based on the fact that I is a function of κ, the EPs can theoretically be located by plotting the change in electrical current as a function of the titrant volume added. The detailed acid-base microtitration procedure used in this work is described in the experimental section. All the experiments were performed using commercial CEa. It should be noted that Joule heating can be detrimental in this method. Indeed, the passage of electrical current through the capillary results in the production of heat and temperature gradients in the buffer solution [20]. If heat is not removed at a rate equal to its production, a progressive temperature rise will occur until a steady state is reached. Both pKa, pH and conductivities are affected by the temperature. In this work, a thermoregulation device that maximize the joule heat dissipation equips the CE apparatus. Moreover, all the experiments were performed at -2 kV in such way that the power (P) generated in the capillary never exceeds 0.5 W/m. This is the best parameter to estimate the intracapillary temperatures. This parameter is given by Eq. 3 [21].

$$\frac{P}{L} = \frac{iV}{L} \quad (3)$$

Where V is the applied voltage, i is the electric current and L is the total capillary length. For an Agilent 7100 CE apparatus, the temperature increases of the electrolyte in the cooled and non-cooled regions of a 50 µm i.d. fused silica capillary (at 0.5 W/m) are respectively 0.88°C and 5.35°C [22]. If we assume that the cooling capacity of the Agilent G1600 3D-CE apparatus is the same, the average temperature of the electrolyte, in the capillary, does not exceed 27.2 °C for all the experiments depicted in this work. It is well known that the conductivity for most ions increases by 2% per kelvin [23]. Then, if we assume that the electric field strength is constant everywhere in the capillary, the maximum error (related to the joule effect) that can be made on the measured electrical current does not exceed 4.4%. To

avoid exceeding 0.5 W/m (for very high conductivity sample) it is recommended to decrease the applied voltage, to dilute the sample or to increase the total capillary length.

As depicted in Table 1, a wide number of acid-base systems characterized either by one or two titratable groups were studied. The titrations were carried out using either strong or weak species as titrant. Fig. 2A' shows the current profiles screen captures obtained for some systems. Other titration curves are in the Supporting Information (Fig. S-1). Moreover, some experiments were performed in hydro-alcoholic media (Systems N-Q in Table 1). For example, in the case of titration of strong base with strong acid (System D in Fig. 2A'), decreasing of the current (in absolute value) is observed until the equivalence point (EP). Beyond this point, the electric current increases (in absolute value) due to the excess of highly mobile hydronium ion in the sample. This profile was obtained by using only 1.1 mL of NaOH (100 µL for each point in the titration curve). In Fig. 2B', the plots of the corrected current intensities ($I_{corr.}$) obtained for different volumes of titrants are shown. For each experiment, the average current intensities recorded from 0.1 to 1 min ($I_{0.1-1\text{min}}$) were corrected for dilution by using Eq. (4) (See recommendations for an accurate reading of the current intensities in Supplementary Fig. 2):

$$I_{corr.} = (I_{0.1-1\text{min}} - I_{res.})\left(\frac{V_0 + V_a}{V_0}\right) \quad (4)$$

Were V_0 is the volume of the titrated solution, V_a the titrant added volume and $I_{res.}$ is the residual current. $I_{res.}$ was evaluated in a blank samples (ultrapure water with resistivity of 18.2 MΩ cm) by using the same methodology (see Fig. S-3 in the supporting information). The intermediate precision of $I_{res.}$ was measured on three different days in eleven replicates. The average $I_{res.}$ obtained over the three days is 0.17 ± 0.05 µA (± 3 × intermediate precision standard deviation). The origin of $I_{res.}$ is not clearly defined. It may arise from many sources such as contamination of water [24] or electronic noise. However, the obtained results, in pure water, suggest that this residual current is nonfaradaic. Indeed, due to the high electrical resistance of the capillary (33 cm of totally length and 50 µm inner diameter) and to the low conductivity of the blank, water electrolysis is unlikely [25]. All the systems described in Table 1 were also characterized by CCT using large sample volumes (100 mL). For a better comparison, titration curves obtained by both methods were normalized on the y-axis (Fig. 2C'). All the titration curves provided by CEa were performed at least three times. As described in Fig. 2C', the curves are almost superimposable. For the determination of the

equivalent points (EPs), the titration curves were splitted into two or three segments (depending of the number of titratable groups). Points close to the equivalence volumes (indicated by black circles in Fig. 2B') were systematically discarded. Moreover, deviations from linearity were also observed during the initial phase of the weak species titrations (Supporting Information Fig. S-1). The nonlinear part of the curves were also excluded. The EPs were determined by setting two trendline equations equal to each other and by calculating the x for which the two lines intersect [26]. For the 17 acid-base systems described in Table 1, the EPs obtained by both methods were compared. The percent relative error (%RE) were calculated by using Eq. (5) [27]:

$$\%RE = \frac{(V_{CEa} - V_{CCT})}{V_{CCT}} 100 \quad (5)$$

where V_{CEa} and V_{CTM} are the equivalence volumes determined by CEa and by CCT, respectively. In Fig. 3, the individual (in circle) and the average %RE (in blue line) are presented. The data related to the systems containing one titratable group are in Fig. 3A while the others are gathered in Fig. 3B. 77 EPs were measured. RE lower than 7% were obtained for the 97.4% of them. The minimal relative standard deviation ($RSD_{n=3}$) value was 0.25% for the system D while the maximal RSD value (n = 3) was 4.94% for the 2nd EP of the system Q. The relative errors are very satisfactory regarding the small volumes used. However, we assume that they can be further reduced by using fluid delivery system with a high accuracy and precision. In this work, the titrant volumes added were determined by gravimetric analysis assuming that the density of the solutions are the same as water. This approximation introduces an additional source of error when the titrant medium is hydro-alcoholic. The electrolysis of water, during the electrophoretic process, has no incidence on the EPs measured by CEa. Indeed, it is well know that the electrochemical oxidation and reduction at the electrodes is inherent to CE [28-32]. Water electrolysis in CE leads to the production of H_3O^+ and OH^- at the electrodes [29-31]. The migration of these ions inside the capillary leads to a drastic increase of the electric current over the time [30]. However, as attested by the 17 current profiles screen captures presented in the Supporting Information (Fig. S-1), no electric current instability was observed in these experimental conditions. First, the displacement of H_3O^+ and OH^- from the electrodes to the ends of the capillary is limited by mass transport (molecular diffusion). Then, a concentration gradient occurs between both ends. Second, the voltage-time product applied is very low (-2 kV min). This is equivalent to an electrokinetic injection of -20 kV during 6 s. The H_3O^+ and OH^- plug lengths introduced are thus insignificant compared to the capillary length. The main limitation of this method is related to

its sensitivity. Due to the electrical current background noise, it may be not appropriate for the titrations of submillimolar analyte concentrations.

CONCLUSION

In this report, it was demonstrated that the commercial CEa can be used, with high confidence, for the end-point detection in microtitration methods. This extends the field of applications and the usefulness of CEa. The EPs can be located by plotting the change in electrical current as a function of the titrant volume added. More interestingly, very low sample volumes (~1.1−1.5 mL of analyte solutions) are required to establish the titration curves. The electrolysis of water, during the electrophoretic process, has no incidence on the EPs measured by CEa. However, the applied voltage during the runs should not exceed -2 kV. RSDs lower than 5% were obtained for the 17 acid-base systems studied with very satisfactory relative errors (< 7% for the 97.4% of the EPs measured). This methodology will be very useful for the titrations of expensive and small sample batch sizes. Application of this strategy for the charge density quantification of nanoparticles is under progress.

Acknowledgements

The authors thank the support of ANR program Labex Arcane (ANR-11-LABX-0003-01).

Appendix A. Supplementary data

Supplementary data associated with this article can be found, in the online version.

References

[1] A. Padarauskas, Electrophoresis 24 (2003) 2054–2063.

[2] Z. Zhu, J. J. Lu, S. Liu, Anal. Chim. Acta 709 (2012) 21–31.

[3] H. Cottet, P. Gareil, Methods Mol. Biol. 384 (2008) 541–567.

[4] F. Oukacine, A. Gèze, L. Choisnard, J. L. Putaux, J. P. Stahl, E. Peyrin, Anal. Chem. 90 (2018) 2493–2500.

[5] F. Oukacine, L. Garrelly, B. Romestand, D. M. Goodall, T. Zou, H. Cottet, Anal. Chem. 83 (2011) 1571–1578.

[6] G. G. Mironov, A. V. Chechik, R. Ozer, J. C. Bell, M. V. Berezovski, Anal. Chem. 83 (2011) 5431–5435.

[7] R. L. C. Voeten, I. K. Ventouri, R. Haselberg, G. W. Somsen, Anal. Chem. 90 (2018) 1464−1481.
[8] R. Vespalec, P. Boček, Chem. Rev. 100 (2000) 3715−3754.
[9] F. Oukacine, S. Bernard, I. Bobe, H. Cottet, J. Control. Release 196 (2014) 139−145.
[10] A. Cifuentes, J. L. Bernal, J. C. Diez-masa, Anal. Chem. 69 (1997) 4271−4274.
[11] Y. François, K. Zhang, A. Varenne, P. Gareil, Anal. Chim. Acta 562 (2006) 164−170.
[12] A. J. Tomlinson, L. M. Benson, N. A. Guzman, S. Naylor, J. Chromatogr. A 744 (1996) 3−15.
[13] C. Canali, L. B. Larsen, Ø. G. Martinsen, A. Heiskanen, Sens. Actuators B Chem. 212 (2015) 544−550.
[14] T. Kaldéus, M. Nordenström, A. Carlmark, L. Wågberg, E. Malmström, Carbohydrate polymers 181 (2018) 871−878.
[15] S. V. Kononova, A. V. Volod'ko, V. A. Petrova, E. V. Kruchinina, Y. G. Baklagina, E. A. Chusovitin, Y. A. Skorik, Carbohydrate Polymers 181 (2018) 86−92.
[16] X. Xu, A. V. Goponenko, S. A. Asher, J. Am. Chem. Soc. 130 (2008) 3113−3119.
[17] F. Mousseau, L. Vitorazi, L. Hermann, S. Mornet, J. F. Berret, J. Colloid Interface Sci. 475 (2016) 36−45.
[18] J. E. Gómez, J. E. Sandoval, Electrophoresis 29 (2008) 381−392.
[19] N. Rodriguez-Laguna, A. Rojas-Hernández, M. T. Ramírez-Silva, L. Hernández-García, M. Romero-Romo, J. Chem. (2015) Article ID 540368.
[20] J. R. Petersen, A. A. Mohammad, Clinical and forensic applications of capillary electrophoresis, Springer Science, New York, 2001.
[21] C. J. Evenhuis, R. M. Guijt, M. Macka, P. J. Mariott, P. R. Haddad, Electrophoresis 26 (2005) 4333−4344.
[22] K. H. Patel, C. J. Evenhuis, L. T. Cherney, S. N. Krylov, Electrophoresis 33 (2012) 1079−1085.
[23] A. Grabowski, Electromembrane desalination processes for production of low conductivity water, Logos Verlag Berlin GmbH, Germany, 2010.
[24] P. T. Kissinger, Curr. Separations 20 (2002) 51−53.
[25] Y. Wang, S. R. Narayanan, W. Wu., ACS Nano 11 (2017) 8421−8428.
[26] J. Garcia, L. D. Schultz, J. Chem. Educ. 93 (2016) 910−914.
[27] K. Siddareddy, M. A. U. Reddy, B. Suresh, J. Sreeramulu, Pharm. Methods 9 (2018) 2−8.

[28] M. Macka, P. Andersson, P. R. Haddad, Anal. Chem. 70 (1998) 743–749.

[29] H. Corstjens, H. A. H. Billiet, J. Frank, K. C. A. M. Luyben, Electrophoresis 17 (1996) 137–143.

[30] A. Timperman, S. E. Tracht, J. V. Sweedler, Anal. Chem. 68 (1996) 2693–2698.

[31] T. Zhu, Y. L. Sun, C.X. Zhang, D. K. Ling, Z. P. Sun, J. High Resolut. Chromatogr. 17 (1994) 563–564.

[32] K. P. Bateman, J. Am. Soc. Mass Spectrom. 10 (1999) 309–317.

Figure 1. Microtitration procedure using commercial CEa.

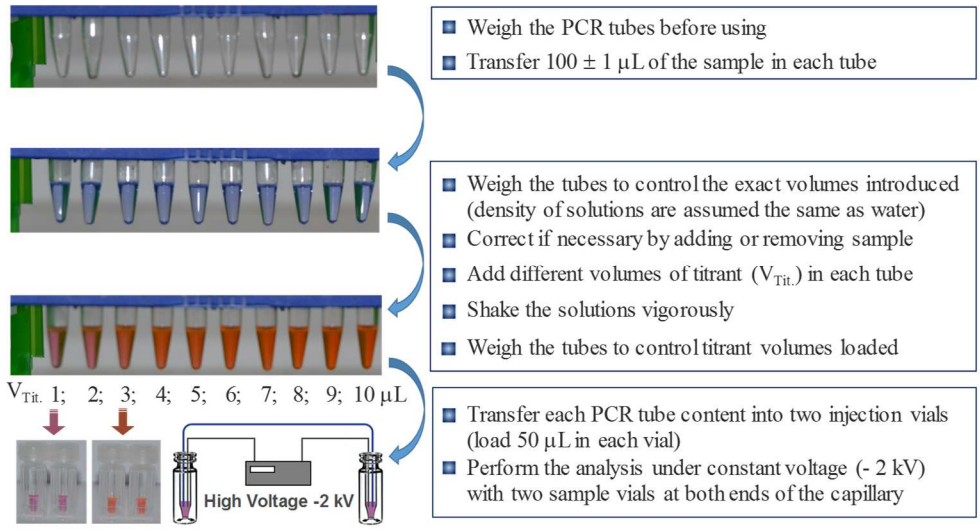

Figure 2. Microtitration of some acid-base systems using commercial CEa. **(A')** Screen captures of the current profiles recorded during the analysis. **(B')** Plots of the corrected current intensities vs volume of the titrants. **(C')** Comparison of the titration curves obtained by conventional conductometric titration (CCT) and by CEa. For a better comparison, titration curves were normalized on the y-axis. All the titration curves obtained by CEa were performed at least three times**.** The experimental conditions are in the experimental section.

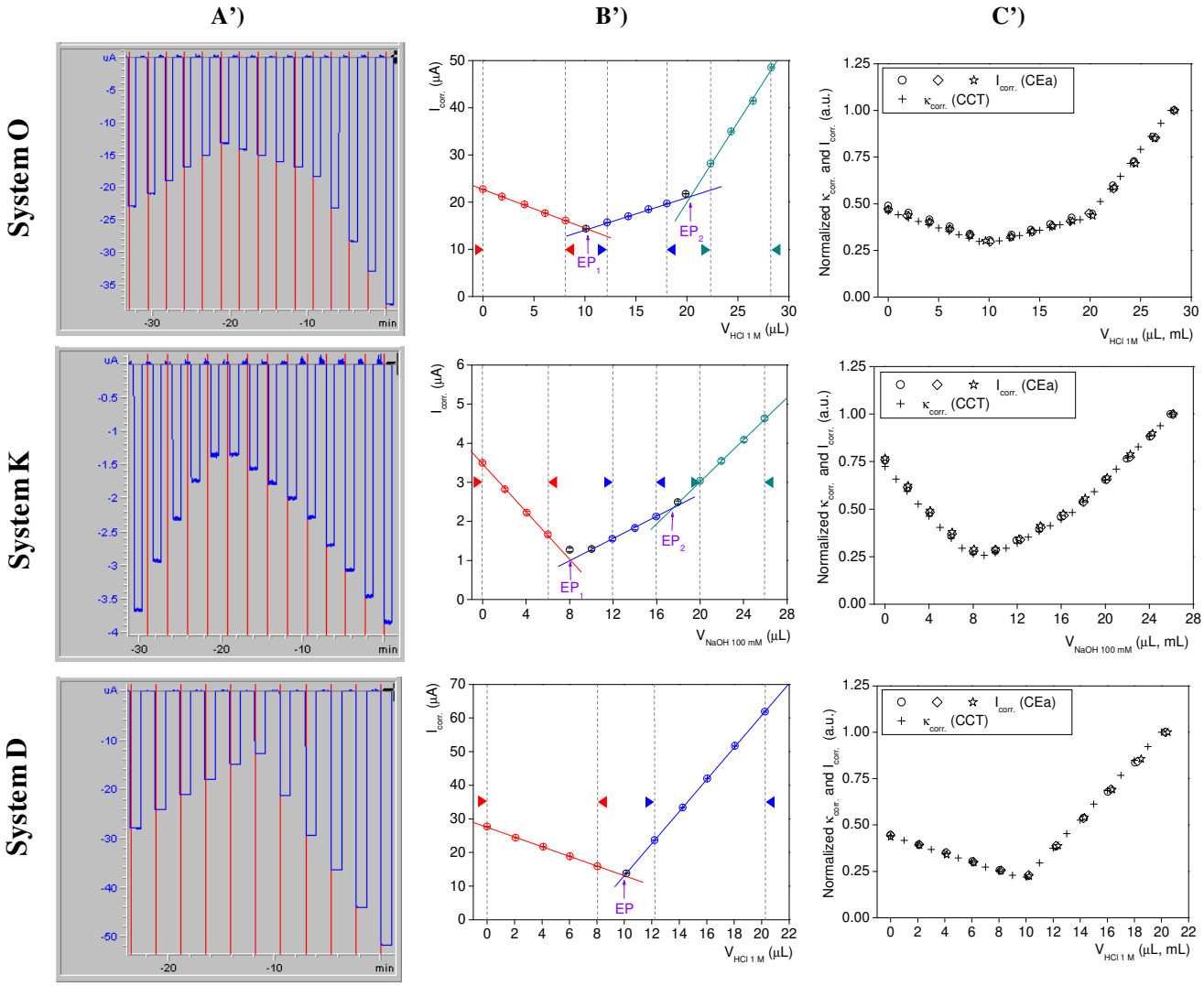

Figure 3. Graphical illustration of the percent relative error (%RE) obtained for the 17 acid-base systems studied (see Table 1). Systems with one (A) and with two titratable groups (B). The experimental conditions are in the experimental section. Abbreviations: EP_1, first equivalent point. EP_2, second equivalent point.

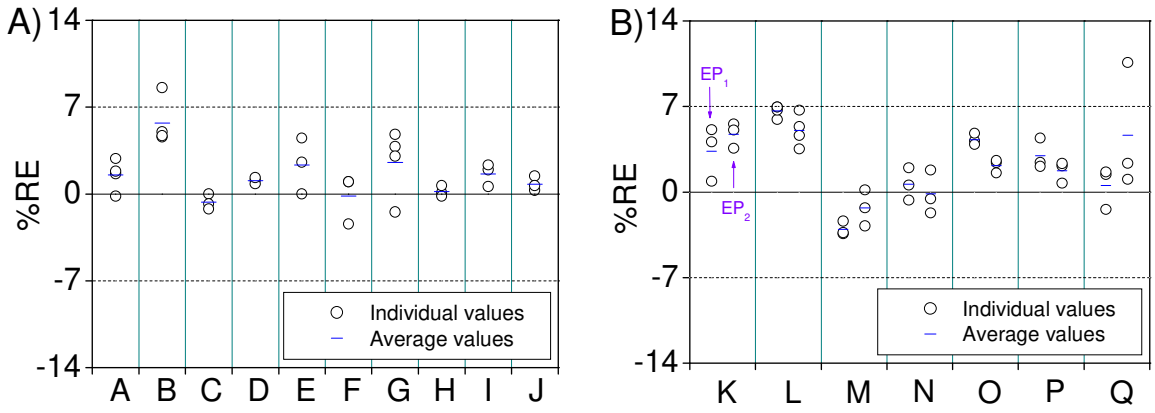

Table 1. Acid-base systems studied in this work.

	Titrated solution	Titrant
(A)	HCl ~ 5 mM	NaOH ~ 100 mM
(B)	HCl ~ 100 mM	NaOH ~ 1 M
(C)	NaOH ~ 5 mM	HCl ~ 100 mM
(D)	NaOH ~ 100 mM	HCl ~ 1 M
(E)	Nicotinic acid ~ 5 mM	NaOH ~ 100 mM
(F)	Nicotinic acid ~ 10 mM	NaOH ~ 100 mM
(G)	Nicotinic acid ~ 100 mM	NaOH ~ 1 M
(H)	Piperidine ~ 100 mM	HCl ~ 1 M
(I)	Tris ~ 5 mM	HCl ~ 100 mM
(J)	Tris ~ 100 mM	HCl ~ 1 M
(K)	Oxalic acid ~ 8 mM	NaOH ~ 100 mM
(L)	Oxalic acid ~ 40 mM	NaOH ~ 1 M
(M)	HCl/CH_3COOH ~ 100/105 mM in KCl 50 mM	NH_4OH ~ 950 mM
(N)	HCl/CH_3COOH ~ 10/11 mM in KCl 31 mM + EtOH 10% (v/v)	NH_4OH ~ 95 mM
(O)	NaOH/Diethanolamine ~ 100/102 mM in KBr 60 mM + EtOH 20% (v/v)	HCl ~ 1 M
(P)	NaOH/ Diethanolamine 6/7 mM in EtOH 20%	HCl ~ 60 mM
(Q)	NaOH/ Diethanolamine 6/7 mM in EtOH 20%	CH_3COOH ~ 60 mM